Microporous Materials

Deutsche Ausgabe: DOI: 10.1002/ange.201509014
Internationale Ausgabe: DOI: 10.1002/anie.201509014

Ionic Covalent Organic Frameworks with Spiroborate Linkage

Ya Du, Haishen Yang[+], Justin Michael Whiteley[+], Shun Wan, Yinghua Jin, Se-Hee Lee, and Wei Zhang**

Abstract: *A novel type of ionic covalent organic framework (ICOF), which contains sp^3 hybridized boron anionic centers and tunable countercations, was constructed by formation of spiroborate linkages. These ICOFs exhibit high BET surface areas up to 1259 $m^2 g^{-1}$ and adsorb a significant amount of H_2 (up to 3.11 wt%, 77 K, 1 bar) and CH_4 (up to 4.62 wt%, 273 K, 1 bar). Importantly, the materials show good thermal stabilities and excellent resistance to hydrolysis, remaining nearly intact when immersed in water or basic solution for two days. The presence of permanently immobilized ion centers in ICOFs enables the transportation of lithium ions with room-temperature lithium-ion conductivity of 3.05×10^{-5} $S cm^{-1}$ and an average Li^+ transference number value of 0.80 ± 0.02. Our approach thus provides a convenient route to highly stable COFs with ionic linkages, which can potentially serve as absorbents for alternative energy sources such as H_2, CH_4, and also as solid lithium electrolytes/separators for the next-generation lithium batteries.*

Covalent organic frameworks (COFs) represent a novel class of porous crystalline organic materials with rigid structures, thermal stabilities, and low densities.[1,2] The two- or three-dimensional architectures of COFs have permanent open channels and accessible voids created by the covalently linked rigid building blocks. COFs have been applied for gas adsorption/separation, catalysis, and electronic devices.[3–6] Most COFs are synthesized through Schiff-base chemistry and boronate ester formation reactions. However, their practical applications have been impeded by the instability of the COFs, particularly in the case of boroxine or boronate ester-containing frameworks.[7] Recently, imine-linked COFs with excellent stability in water, acid, and base have been developed through introduction of certain substituents (e.g. OH or OMe) into the backbone structures.[8,9] Spiroborates are ionic derivatives of boronic acid which have been reported to exhibit high resistance toward hydrolysis and be stable in water, methanol, and under basic conditions.[10,11] In addition, given the ionic character, COFs linked by spiroborates have the potential to function as ion conductive materials.[12–17] The spiroborate linkage can be formed readily through the condensation of polyols with alkali tetraborate,[11,18–20] or boric acid,[21–23] or through the transesterification between borate and polyols[10] in a thermodynamic manner. Previously, spiroborate linkages have been successfully used in the construction of macrocycles[10,22,24–25] which show interesting applications as electrolytes,[26] sensors,[23,27] catalysts,[28] and hosts of neutral molecules or ions.[22,29,30] Although the spiroborate formation is reversible, stable, and easily accessible, thus suitable for construction of COFs, it has not yet been explored in the synthesis of COFs. Herein, we present the design and synthesis of porous spiroborate-linked ionic COFs (ICOFs) that exhibit excellent stability in water, high uptake of H_2 and CH_4, and also high room-temperature ion conductivity.

First, we studied the transesterification of diol **1** and trimethyl borate as a model reaction. The formation of spiroborate linkages proceeds with release of a proton and thus is favored in the presence of proton acceptors. Therefore, we examined the reaction in the presence of dimethyl amine. We observed nearly complete conversion of diol **1** to the product **2** within 60 minutes at room temperature (see Figure S1 in the Supporting Information), while a much more sluggish reaction was observed in the absence of a base.

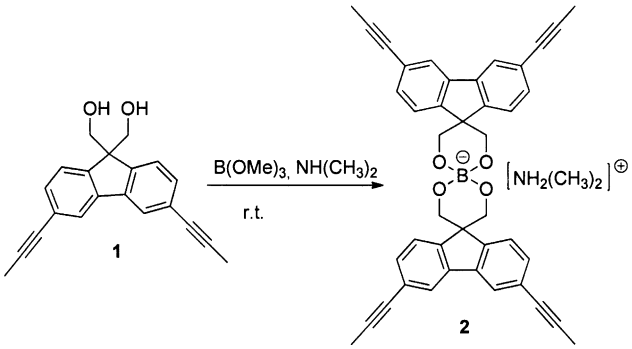

Encouraged by this result, we then examined the possibility to generate COFs linked by spiroborates. We designed a D_4-symmetric macrocycle **5** equipped with four diol groups as a multifunctional building block. Macrocycle **5** was readily obtained from compound **3** in two steps through alkyne metathesis cyclo-oligomerization[31] followed by deprotection (Scheme 1). The polyol building blocks reported for COFs so far have been mainly limited to polyfunctional catechol derivatives. Therefore, shape-persistent macrocycles employed herein represent a new type of nanosized building

[*] Dr. Y. Du, Dr. H. Yang,[+] Dr. Y. Jin, Prof. Dr. W. Zhang
Department of Chemistry and Biochemistry
University of Colorado, Boulder, CO 80309 (USA)
E-mail: wei.zhang@colorado.edu
J. M. Whiteley,[+] Prof. Dr. S. Lee
Department of Mechanical Engineering
University of Colorado, Boulder, CO 80309 (USA)
Dr. S. Wan
Storagenergy Technologies, Inc.
Salt Lake City, UT 84120 (USA)
[+] These authors contributed equally to this work.
Supporting information for this article is available on the WWW under http://dx.doi.org/10.1002/anie.201509014.

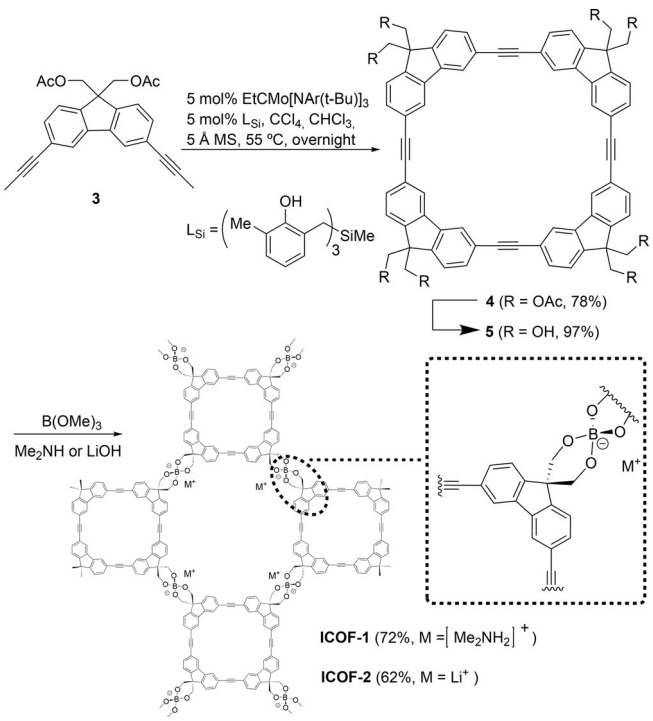

Scheme 1. Synthesis of **ICOF-1** and **ICOF-2**.

blocks, which contain preexisting non-collapsible internal cavities.

We then tested the formation of spiroborate-linked COFs through the condensation of **5** and trimethyl borate under similar conditions to the model study. We used dimethylformamide (DMF) as the solvent, in which the polyol **5** has decent solubility. The reaction was carried out at 120 °C for 7 days in nitrogen atmosphere. A gray gel was formed gradually during the reaction, which was collected by centrifugation and washed with acetone to yield **ICOF-1** (72 %). One of the advantages of ionic spiroborate linkage is the easy tunability of counterions, which could have profound effect on the materials properties, such as gas adsorption capacity and ion conductivity. By using LiOH as the base instead of dimethyl amine, a framework with lithium counterion (**ICOF-2**) was obtained in decent yield (62 %) under otherwise identical conditions.

ICOF-1 and **ICOF-2** were characterized by FT-IR and ^{13}C magic-angle spinning (MAS) NMR spectroscopy, elemental analysis, thermogravimetric analysis (TGA), scanning electron microscopy (SEM), and powder X-ray diffraction (PXRD) analysis. The FT-IR spectra (Figure S2) of **ICOF-1** and **ICOF-2** show the absorption bands, respectively, at 1401 and 1435 cm^{-1}, which are characteristic for the stretching of the borate ester bond (B–O). A similar B–O stretching band (1418 cm^{-1}) was also observed in the IR spectrum of model compound **2**. The O–H stretch from the hydroxy groups of macrocycle **5** is nearly absent in the IR spectrum of **ICOF-2**, indicating the successful formation of spiroborate linkages from diol functional groups of **5**. The broad absorption band around 3410 cm^{-1} in the IR spectrum of **ICOF-1** likely corresponds to the NH stretch of the $[NH_2Me_2]^+$ counterion. In the MAS solid-state ^{13}C NMR spectrum of **ICOF-1** (Figure S3), we observed singlets at 90.1, 70.2, and 54.5 ppm, corresponding to the ethynylene carbon atoms, methylene carbon next to the hydroxy groups, and the quaternary carbon in the fluorene ring, respectively. The carbon resonance of $[Me_2NH_2]^+$ was observed as a singlet at 38.6 ppm. Solid-state ^{13}C NMR spectra of **ICOF-2** (Figure S4) shows similar singlets at 90.9, 72.1, and 52.9 ppm, but with the absence of the peak around 38.6 ppm, supporting the replacement of $[Me_2NH_2]^+$ with lithium cations. The thermogravimetric analysis (TGA, Figure S8) shows a very gradual onset of the weight loss, and precise measurement of the onset temperature was difficult. Nevertheless, both ICOFs exhibit good thermal stability, showing weight loss of 7–12 % at 400 °C in nitrogen atmosphere. SEM images of **ICOF-1** and **ICOF-2** support their single-crystalline morphology (Figures S12 and S13). The PXRD characterization (Figure 1, and S11) of

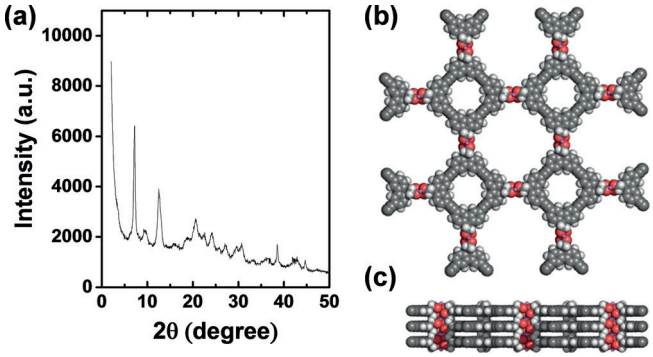

Figure 1. PXRD patterns of **ICOF-2** (a), proposed structural representations of **ICOF-2**, top view (b), side view (c).

ICOF-1 and **ICOF-2** shows multiple peaks in the 2θ range of 2–35° indicating certain structure orderliness in the framework. The base used in the reaction affects the crystallinity of the resulting ICOFs, presumably because of their different size, solubility in the reaction medium, and also counter cation effect. When LiOH with low solubility in the reaction medium is used as the base, the resulting **ICOF-2** shows better crystallinity. We attempted to convert **ICOF-1** to more crystalline **ICOF-2** through the exchange of counter cations by soaking the framework in 1 M LiOH solution. However, we only observed significant BET surface area decrease of **ICOF-1** (1022 m^2 g^{-1} vs. 210 m^2 g^{-1}) without improvement of crystallinity (Figure S10). Because of the complex diffraction patterns and the limited quality and resolution of the data, we were unable to simulate the crystal packing. The proposed 2D structural representations of **ICOF-2** are shown in Figure 1 b, and 1 c.

The gas adsorption properties of ICOFs were then investigated with freshly activated samples. Prior to the porosity measurements, all the samples were degassed in dynamic vacuum for 24 h at 100 °C. As shown in Figure 2 a, **ICOF-1** shows typical type I adsorption behavior at 77 K with a rapid uptake at low relative pressure ($P/P_0 < 0.01$), indicating its permanent microporous nature. In contrast, the isotherm of **ICOF-2** is the intermediate of type I and type IV, showing more pronounced continuous uptake

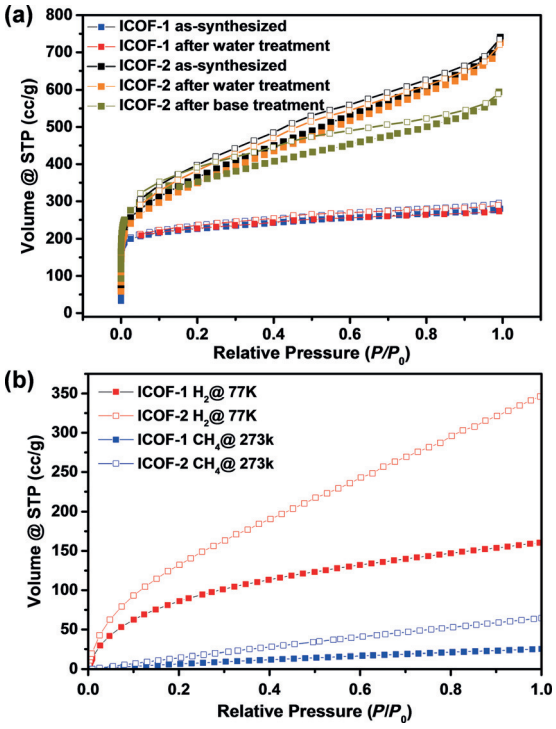

Figure 2. a) Nitrogen gas adsorption isotherms for **ICOF-1** and **ICOF-2** measured at 77 K. Filled symbols represent adsorption and hollow symbols represent desorption. b) Hydrogen and methane adsorption isotherms.

beyond $P/P_0 = 0.05$ with apparent hysteresis. The non-local density functional theory (NLDFT) pore-size distribution analysis shows that **ICOF-1** has micropores centered around 1.1 nm, while **ICOF-2** has mesopores centered around 2.2 nm together with larger mesopores in the range of 2–6 nm (Figure S7). Brunauer–Emmett–Teller (BET) surface areas of **ICOF-1** and **ICOF-2** are 1022 and 1259 $m^2 g^{-1}$, respectively.

It has been reported that doping of COFs with alkali metals (Li, Na, and K) can dramatically increase the hydrogen uptake by increasing the gas binding energy.[32] **ICOF-2** containing a Li^+ counterion is thus examined for the adsorption of alternative energy source, hydrogen, and methane. As expected, it shows excellent adsorption capacities towards H_2 (3.11 wt%, 77 K, 1 bar) and CH_4 (4.62 wt%, 273 K, 1 bar), which are among the highest in all organic porous materials that have been reported, and even competitive with the best reported MOFs under the same conditions.[33] We observed more than two-fold decreases of the H_2 and CH_4 uptakes in **ICOF-1** compared to **ICOF-2** (Figure 2b), which suggests that the metal cations play a significant role in improving the gas uptake. Our approach (i.e. ionic spiroborate formation) thus represents an interesting alternative strategy for doping of COFs with metal cations to maximize the adsorption of hydrogen.

Commonly used boronate ester (or boroxine) linkages in COF synthesis contain Lewis acidic boron centers, which are often prone to hydrolytic decomposition even in atmospheric moisture at ambient temperature. It is anticipated that the additional Lewis base coordination to boron in anionic spirocyclic esters makes the hydrolysis reaction less favorable. The stability of ICOFs toward hydrolysis was thus investigated. To our delight, both **ICOF-1** and **ICOF-2** show great stability in water. No significant changes in the BET surface areas and PXRD spectra were observed between the samples before and after immersion in water for 2 days (Figure 2a). **ICOF-2** also exhibits good stability under basic condition (1 M LiOH, 2 days), showing similar PXRD spectrum and slight decrease in BET surface area (1259 vs. 1105 $m^2 g^{-1}$) compared to those of the fresh sample before the base treatment. We did not observe any organic residues remaining in the water and base solutions after the treatment, which further confirms the excellent hydrolytic stability of ICOFs. Although we still did not collect any soluble residues in the aqueous phase after the treatment with stronger bases, **ICOF-2** shows decrease of the surface area: 8% decrease when stirred in 6 M LiOH, for 24 h, and a 72% decrease when stirred in 12 M LiOH for 24 h. Both ICOFs are unstable in aqueous acidic solution, because of the acid-labile nature of spiroborates.

Given the unique porous and ionic nature of these ICOFs, the Li^+-containing **ICOF-2** is envisioned as a Li-conducting solid electrolyte, advantageously being lightweight and possessing high thermal and chemical stability. Thus, we next tested the ion conductivity of ICOFs. **ICOF-2** microcrystals were mixed with polyvinylidene fluoride (PVDF) in a 2 to 1 weight ratio in *N*-methyl-2-pyrrolidone (NMP) and subsequently bladed onto aluminum foil. The film (**ICOF-2**:PVDF) was dried at 80 °C overnight eventually peeling off the aluminum to form a freestanding membrane. Discs of $\Phi =$ 1.3 cm were punched from the dried film and further dried at 120 °C in vacuum to remove any residual moisture and NMP. Discs were then soaked in propylene carbonate (PC) for 24 hours before characterization.[34,35] The PC content in **ICOF-2**:PVDF was approximately 55 wt% based on thermogravimetric analysis. Nyquist plots (Figure 3a) of the

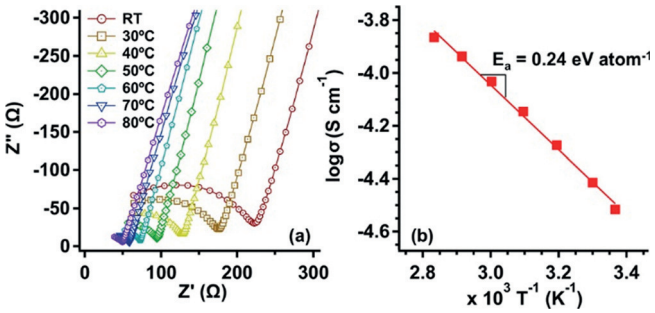

Figure 3. Electrochemical tests performed on **ICOF-2**:PVDF films. a) Nyquist plot of AC impedance sweeps at various temperatures. b) Ionic conductivity as a function of temperature.

ICOF-2:PVDF sample show a steep tail at low frequency, confirming the capacitive nature of the electrode/electrolyte interface. Thus a suitable contact was made with the lithium-ion blocking electrodes.[36] A room-temperature conductivity of 3.05×10^{-5} S cm^{-1} was observed.[34,37] No conductivity contribution is expected from PVDF or PC. Because of the frequency and temperature range, contributions could not be separated between grain boundary and bulk conductivity, however, both are included in determining overall conduc-

tivity as shown in the Arrhenius plot of Figure 3b. In contrast to classic polymer electrolytes, which show non-linear activation energy at higher temperatures, **ICOF-2** exhibits the linear characteristic of conductivity with temperature, which is typical of ceramic solid conductors. The activation energy of **ICOF-2** is 0.24 eV atom^{-1}, a favorable value and comparable to some of the best crystalline solid electrolytes.[38] An average Li^+ transference number value of 0.80 ± 0.02 was determined for **ICOF-2** using the Bruce–Vincent–Evans (BVE) method (Figure S14c). This value is significantly higher than those for typical solid-state polymer electrolytes with dopant lithium salt, which are generally in the range of 0.2–0.5.[39] It should be noted that lithium ions are not dissolving into the PC to act as a liquid electrolyte, as typical liquid electrolytes have lithium ion transference numbers on the order of 0.50. The large resistance increase is most likely from the passivation from the PC on lithium surface.[40]

A linear sweep voltammetry (LSV) measurement of **ICOF-2**:PVDF shows a general sloping profile between 0.2 to 4 V because of the resistive nature of the **ICOF-2**:PVDF membrane at room temperature (Figure S14d). At above 4.5 V, PC breaks down with lithium, leading to an increase in the observed current. This demonstrates potential compatibility of ICOFs with current high-voltage cathode materials.

In conclusion, we have developed a novel type of ionic COFs linked by spiroborate, which exhibit high surface areas and good thermal stability. The ionic COFs show excellent uptake of H_2 (3.11 wt%, 77 K, 1 bar) and CH_4 (4.62 wt%, 273 K, 1 bar), comparable to the highest adsorption capacity reported so far for COFs. By virtue of the ionic borate linkage, ICOFs enable the transportation of lithium ions, suggesting their potential applications as solid electrolytes. The advantages of these ICOFs include their great resistance to hydrolysis and easy tunability of counter cations, which would have a profound effect on their properties, such as porosity, gas adsorption capacity and selectivity, and ion transport capability. Our strategy involving spiroborate formation provides new possibilities for preparing porous materials with novel ionic structures and intriguing properties.

Acknowledgements

The authors thank the National Science Foundation (grant number DMR-1055705), Dr. Matthew Cowan for help with TGA measurement, Sarah M. Dischinger for PXRD data collection, and Prof. Richard Shoemaker for assistance in solid-state NMR characterization.

Keywords: covalent organic frameworks · gas adsorption · ionic polymers · lithium-ion conductivity · spiroborates

How to cite: *Angew. Chem. Int. Ed.* **2016**, *55*, 1737–1741
Angew. Chem. **2016**, *128*, 1769–1773

[1] H. M. El-Kaderi, J. R. Hunt, J. L. Mendoza-Cortés, A. P. Côté, R. E. Taylor, M. O'Keeffe, O. M. Yaghi, *Science* **2007**, *316*, 268–272.
[2] A. P. Côté, A. I. Benin, N. W. Ockwig, M. O'Keeffe, A. J. Matzger, O. M. Yaghi, *Science* **2005**, *310*, 1166–1170.
[3] X. Feng, X. S. Ding, D. L. Jiang, *Chem. Soc. Rev.* **2012**, *41*, 6010–6022.
[4] S. Y. Ding, W. Wang, *Chem. Soc. Rev.* **2013**, *42*, 548–568.
[5] J. W. Colson, W. R. Dichtel, *Nat. Chem.* **2013**, *5*, 453–465.
[6] F. J. Uribe-Romo, W. R. Dichtel, *Nat. Chem.* **2012**, *4*, 244–245.
[7] L. M. Lanni, R. W. Tilford, M. Bharathy, J. J. Lavigne, *J. Am. Chem. Soc.* **2011**, *133*, 13975–13983.
[8] H. Xu, J. Gao, D. Jiang, *Nat. Chem.* **2015**, *7*, 905–912.
[9] S. Kandambeth, A. Mallick, B. Lukose, M. V. Mane, T. Heine, R. Banerjee, *J. Am. Chem. Soc.* **2012**, *134*, 19524–19527.
[10] B. F. Abrahams, D. J. Price, R. Robson, *Angew. Chem. Int. Ed.* **2006**, *45*, 806–810; *Angew. Chem.* **2006**, *118*, 820–824.
[11] H. C. Brown, M. V. Rangaishenvi, *J. Organomet. Chem.* **1988**, *358*, 15–30.
[12] S. Chandra, T. Kundu, S. Kandambeth, R. BabaRao, Y. Marathe, S. M. Kunjir, R. Banerjee, *J. Am. Chem. Soc.* **2014**, *136*, 6570–6573.
[13] S. Jin, et al., *Angew. Chem. Int. Ed.* **2013**, *52*, 2017–2021; *Angew. Chem.* **2013**, *125*, 2071–2075.
[14] S. Wan, J. Guo, J. Kim, H. Ihee, D. L. Jiang, *Angew. Chem. Int. Ed.* **2008**, *47*, 8826–8830; *Angew. Chem.* **2008**, *120*, 8958–8962.
[15] S. Wan, J. Guo, J. Kim, H. Ihee, D. L. Jiang, *Angew. Chem. Int. Ed.* **2009**, *48*, 5439–5442; *Angew. Chem.* **2009**, *121*, 5547–5550.
[16] C. R. DeBlase, K. E. Silberstein, T.-T. Truong, H. D. Abruña, W. R. Dichtel, *J. Am. Chem. Soc.* **2013**, *135*, 16821–16824.
[17] J. F. Van Humbeck, M. L. Aubrey, A. Alsbaiee, R. Ameloot, G. W. Coates, W. R. Dichtel, J. R. Long, *Chem. Sci.* **2015**, *6*, 5499–5505.
[18] M. Van Duin, J. A. Peters, A. P. G. Kieboom, H. Van Bekkum, *Tetrahedron* **1985**, *41*, 3411–3421.
[19] M. Van Duin, J. A. Peters, A. P. G. Kieboom, H. Van Bekkum, *Tetrahedron* **1984**, *40*, 2901–2911.
[20] K. Yoshino, M. Kotaka, M. Okamoto, H. Kakihana, *Bull. Chem. Soc. Jpn.* **1979**, *52*, 3005–3009.
[21] E. Voisin, T. Maris, J. D. Wuest, *Cryst. Growth Des.* **2008**, *8*, 308–318.
[22] H. Danjo, K. Hirata, S. Yoshigai, I. Azumaya, K. Yamaguchi, *J. Am. Chem. Soc.* **2009**, *131*, 1638–1639.
[23] N. Kameta, K. Hiratani, *Tetrahedron Lett.* **2006**, *47*, 4947–4950.
[24] Y. Loewer, C. Weiss, A. T. Biju, R. Froehlich, F. Glorius, *J. Org. Chem.* **2011**, *76*, 2324–2327.
[25] H. Danjo, N. Mitani, Y. Muraki, M. Kawahata, I. Azumaya, K. Yamaguchi, T. Miyazawa, *Chem. Asian J.* **2012**, *7*, 1529–1532.
[26] M. Moriya, D. Kato, W. Sakamoto, T. Yogo, *Chem. Commun.* **2011**, *47*, 6311–6313.
[27] N. Kameta, K. Hiratani, *Chem. Commun.* **2005**, 725–727.
[28] C. Carter, S. Fletcher, A. Nelson, *Tetrahedron: Asymmetry* **2003**, *14*, 1995–2004.
[29] H. Danjo, T. Nakagawa, K. Katagiri, M. Kawahata, S. Yoshigai, T. Miyazawa, K. Yamaguchi, *Cryst. Growth Des.* **2015**, *15*, 384–389.
[30] H. Danjo, K. Hirata, M. Noda, S. Uchiyama, K. Fukui, M. Kawahata, I. Azumaya, K. Yamaguchi, T. Miyazawa, *J. Am. Chem. Soc.* **2010**, *132*, 15556–15558.
[31] W. Zhang, J. S. Moore, *J. Am. Chem. Soc.* **2005**, *127*, 11863–11870.
[32] J. L. Mendoza-Cortés, S. S. Han, W. A. Goddard, *J. Phys. Chem. A* **2012**, *116*, 1621–1631.
[33] M. P. Suh, H. J. Park, T. K. Prasad, D.-W. Lim, *Chem. Rev.* **2012**, *112*, 782–835.
[34] A. Anani, S. Crouchbaker, R. A. Huggins, *J. Electrochem. Soc.* **1987**, *134*, 3098–3102.
[35] R. Ameloot, M. Aubrey, B. M. Wiers, A. P. Gomora-Figueroa, S. N. Patel, N. P. Balsara, J. R. Long, *Chem. Eur. J.* **2013**, *19*, 5533–5536.

[36] W. B. Reid, E. E. Lachowski, A. R. West, *Phys. Chem. Glasses* **1990**, *31*, 103 – 108.
[37] B. M. Wiers, M. L. Foo, N. P. Balsara, J. R. Long, *J. Am. Chem. Soc.* **2011**, *133*, 14522 – 14525.
[38] N. Kamaya, et al., *Nat. Mater.* **2011**, *10*, 682 – 686.
[39] E. Quartarone, P. Mustarelli, *Chem. Soc. Rev.* **2011**, *40*, 2525 – 2540.
[40] E. Cattaneo, B. Rasch, W. Vielstich, *J. Appl. Electrochem.* **1991**, *21*, 885 – 894.

Received: September 25, 2015
Published online: December 23, 2015

